THE ASTROPHYSICAL JOURNAL, 466:713–723, 1996 August 1

SEYFERT GALAXIES. IV. NUCLEAR PROFILES OF MARKARIAN SEYFERT GALAXIES FROM *HUBBLE SPACE TELESCOPE* IMAGES[1]

CHARLES H. NELSON AND JOHN W. MACKENTY
Space Telescope Science Institute, 3700 San Martin Drive, Baltimore, MD 21218; cnelson@stsci.edu; mackenty@stsci.edu
SUSAN M. SIMKIN
Michigan State University, Department of Physics and Astronomy, East Lansing, MI 48824-1116; simkin@grus.pa.msu.edu
AND
RICHARD E. GRIFFITHS
Johns Hopkins University, Physics and Astronomy, 3400 North Charles Street, Baltimore, MD 21218; griffith@mds.pha.jhu.edu
Received 1995 September 18; accepted 1996 February 14

ABSTRACT

We have examined the nuclear profiles of the Seyfert and non-Seyfert Markarian galaxies in our near-infrared *Hubble Space Telescope* WF/PC-1 snapshot survey. We find that nuclei of types 1–1.5 Seyfert galaxies are dominated by strong point sources, while those of Seyfert 2 and non-Seyfert Markarian galaxies tend to be resolved, less distinguished, and similar in shape to normal galaxy luminosity profiles. Two possible interpretations of this result for type 2 Seyfert galaxies are that their nuclear continuum sources are undetected in our bandpass, contributing less than 10% of the nuclear light (within 0.″5 radius) in all cases or that their nuclear components are resolved and blend in smoothly with the brightness profile of the host galaxy's bulge. Since spectroscopic studies support typical nuclear continuum fractions distinctly greater than 10%, the latter conclusion is clearly preferable. If the continua observed in Seyfert 2 galaxies originate as nuclear light that is redirected into the line of sight by scattering, as predicted by unified models of active galactic nuclei, then the scattering regions must be extended. Simple simulations suggest that these regions must cover several tens of parsecs or more, in agreement with estimates of the sizes of the scattering "mirrors" in other Seyfert 2 galaxies. However, the similarity of the profiles of non-Seyfert Markarian and type 2 Seyfert nuclei suggests that circumnuclear star formation may also be an important component in the nuclear profiles of the latter.

Subject headings: galaxies: nuclei — galaxies: photometry — galaxies: Seyfert

1. INTRODUCTION

In unified models for active galactic nuclei (AGNs), two kinematically and spatially distinct regions of gaseous emission surround a central ionizing continuum source. The broad line region (BLR) emits extremely broad permitted emission lines with widths (FWHM) up to 10,000 km s^{-1}. In the narrow line region (NLR), significantly narrower permitted and forbidden lines are produced with widths of a few hundred km s^{-1}. Studies of the polarization properties and variability of the BLR and the continuum indicate that these components are interior to the NLR on scales less than a parsec in diameter (Peterson 1993; Antonucci 1993), while the NLR can extend to radii as large as 1 kpc.

Unified models are based on the idea that in certain objects emission from the continuum source and BLR are blocked by a torus composed of dense molecular clouds (see, e.g., Antonucci 1993). This obscuring torus has an inner radius that is comparable to the size of the BLR and has a symmetry axis that is independent of the orientation of the galactic disk, instead aligning with the kiloparsec-scale radio source, when present. Seyfert galaxies are classified on the basis of the visibility of the BLR and continuum source with respect to the NLR features. In the unified model, if the torus is effectively face on, we get a clear view of the BLR and nuclear continuum, and the galaxy displays Seyfert 1 characteristics. In Seyfert 2 galaxies these regions are blocked, and only NLR features are visible. A sequence of intermediate classes are also found, types 1.5, 1.8, and 1.9, in which the prominence of the BLR and nuclear continuum source decreases.

The detection of broad permitted lines in polarized light in a growing number of Seyfert 2 galaxies has given considerable support for unified models (Antonucci & Miller 1985; Miller & Goodrich 1990; Tran 1995a). These lines and also the relatively weak nuclear continua observed in Seyfert 2 galaxies have been scattered into our line of sight by material that is directly exposed to the nuclear emissions, presumably lying directly above the torus in an extended conical region with opening angles ranging between 40° and 100° (Wilson 1995). Since the degree of continuum polarization appears to be independent of frequency, this material is thought to be largely free electrons, although contributions from dust scattering are also possible, especially at larger distances from the nucleus. Observations suggest that these scattering "mirrors" are likely to be extended, covering a region of as much as 1″ in the case of NGC 1068 (see Antonucci 1993), corresponding to roughly 100 pc.

In this paper we test the expectations from the unified model by examining the nuclear profile shapes in our *HST*

[1] Based on observations with the NASA/ESA *Hubble Space Telescope* obtained at the Space Telescope Science Institute, which is operated by Association of Universities for Research in Astronomy, Inc., under NASA contract NAS 5-26555.

snapshot survey of Seyfert and non-Seyfert Markarian galaxies. Our observations were made in a bandpass that is virtually free of emission lines, and so our images represent the distribution of starlight and other continuum emission processes. We can therefore test whether the continuum sources in Seyfert 2 nuclei are extended while Seyfert 1 nuclei are unresolved, as expected in unified models. In the next section we briefly describe the observations and reductions. In § 3 we present our results. In § 4 we discuss the strength and shape of the nuclei in Seyfert 1 and 2 galaxies in terms of the unified models of AGNs, and we summarize our conclusions in § 5.

2. SAMPLE AND OBSERVATIONS

We have obtained *Hubble Space Telescope* (*HST*) images of a sample of 52 Markarian Seyfert galaxies and a comparison sample of 48 non-Seyfert Markarian galaxies. Both samples are listed in MacKenty (1989, hereafter Paper II), and ground-based imaging of the Seyfert sample has been presented in MacKenty (1990, hereafter Paper I). Essentially all Markarian Seyfert galaxies known as of 1983 with recession velocities between 3000 and 13,000 km s^{-1}, $M_{pg} < -19$ ($H_0 = 75$ km s^{-1} Mpc^{-1} assumed throughout), $m_{pg} < 16.5$, and declinations between $-20°$ and $+60°$ are included (two objects, Mrk 248 and Mrk 280, were not observed, the first because of a missed target and the second due to instrument safing). Also seven NGC galaxies with apparent magnitudes brighter than the limit of the Markarian survey were added. This is as close to a complete sample of luminous Seyfert galaxies as can be constructed while maintaining a sufficiently large number of galaxies to properly represent this diverse population.

The *HST* observations are described in detail in MacKenty et al. (1996, hereafter Paper III). Briefly, short exposures of the inner regions of each galaxy were made using the *HST* Wide Field Planetary Camera (WF/PC-1; Westphal et al. 1982) in "snapshot" mode. The data were calibrated with the standard pipeline processing (Lauer 1989; MacKenty et al. 1992) and were deconvolved with the accelerated Lucy algorithm (Lucy 1974; Richardson 1972) as implemented in STSDAS. The galaxy nuclei were placed in the center of the PC6 detector, and coarse track guiding was employed producing a pixel scale of 43 mas $pixel^{-1}$ and a spacecraft rms motion (or jitter) of 15–80 mas. For the range of redshifts in our sample, these images have resolutions of 20–80 pc and typically provide good signal to noise out to better than 1 kpc from the nucleus. The observations were made using the F785LP filter to image the stellar continuum in a bandpass virtually free of emission lines and containing low internal absorption. This broadband filter has a sharp cut-on at about 7800 Å, a central wavelength of 8876 Å and extends to ~ 1 μm at the sensitivity limit of the CCD detectors (MacKenty et al. 1992).

3. RESULTS

In the process of inspecting our images we noticed a striking difference in the appearances of types 1 and 2 Seyfert nuclei. There was an obvious tendency for the type 1 nuclei to be dominated by a strong point source showing the characteristic pattern of the *HST* aberrated point spread function. By contrast, the nuclei of type 2 Seyfert galaxies were considerably less prominent, and *none* displayed the typical point source signature. This dichotomy is demonstrated in Figure 1, which shows the undeconvolved nuclei of a Seyfert 1, Mrk 618 (*top*), and a Seyfert 2, Mrk 622 (*bottom*).

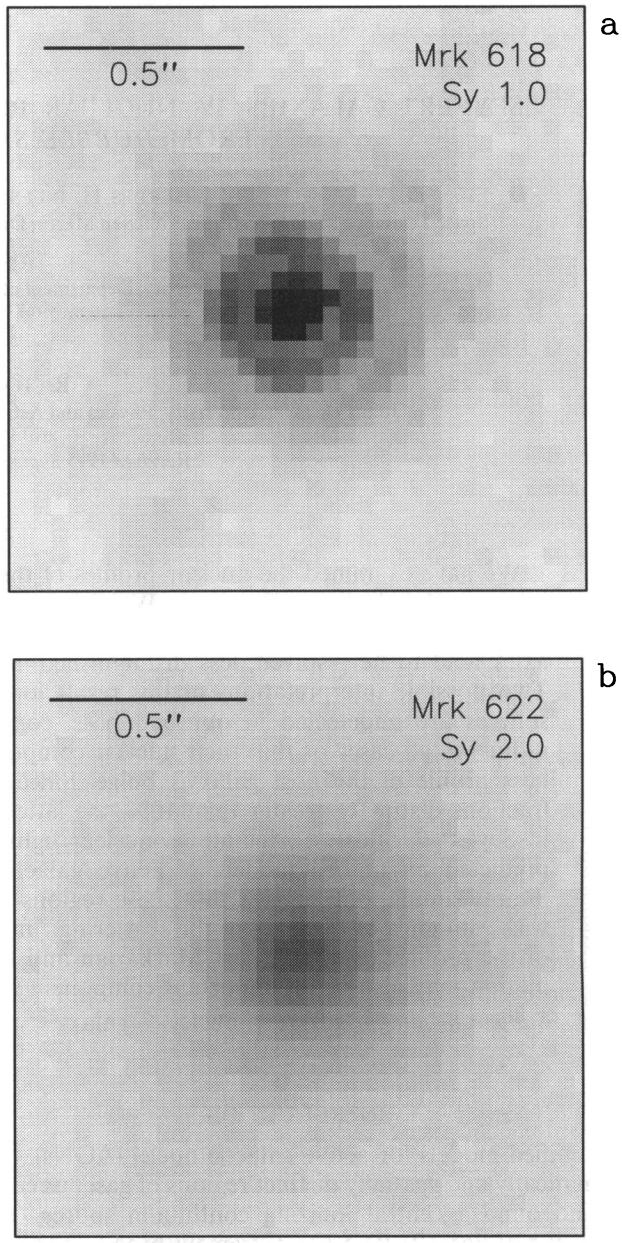

FIG. 1.—Nuclear regions of the type 1 Seyfert, Mrk 618 (*top*) and the type 2 Seyfert, Mrk 622 (*bottom*), are shown to illustrate the general difference in appearance of the two classes. Note the ring at ~ 4 pixels and the other features in the type 1 typical of an unresolved source in contrast to the "soft" nucleus of the Seyfert 2.

The nuclei of the Seyfert 1 galaxies could also be distinguished numerically by the deconvolution algorithms, which left artifacts such as residual rings and spikes extending over 40 pixels from the center because of the undersampling in the image (indicating that the nucleus was a true point source with a size less than 43 mas). Such difficulties were rarely encountered with the Seyfert 2 and non-Seyfert Markarian nuclei.

3.1. *Qualitative Classification: NPC*

To approach this distinction in a systematic way we first devised a *qualitative* classification scheme that differentiates

TABLE 1

NUCLEAR PROMINENCE CLASS

Class	Feature
0.....	No clear nucleus; irregular galaxy
1.....	Soft, weak resolved nucleus
2.....	Stronger nucleus; elongated or slightly resolved
3.....	Sharp point source but not overly luminous
4.....	Dominant unresolved nucleus

objects based on the appearance of the nucleus. The nuclear prominence class, hereafter NPC, indicates increasing strength of the nuclear point source on a scale from 0 to 4 (the specific definition of each level is given in Table 1). The values of NPC and other parameters used in this paper are given in Tables 2A–2B for each galaxy and were assessed from deconvolved images.

In Figure 2 we present histograms of NPC separated by nuclear activity type. There is a strong tendency for Seyfert

TABLE 2

A. NUCLEAR PROFILE PARAMETERS FOR MARKARIAN SEYFERT GALAXIES

Name	Sy Type	cz km/s	*NPC*	*W*(2) pix	*W*(6) pix	*P*(2) DN	*P*(6) DN	*S*(2) (×100)	*S*(6)
(1)	(2)	(3)	(4)	(5)	(6)	(7)	(8)	(9)	(10)
Mrk 9	1.0	12040	4	2.4	4.3	1922	1596	9.03	1.63
Mrk 50	1.0	6910	4	3.8	5.5	317	278	8.08	1.22
Mrk 79	1.5	6580	4	2.5	4.5	3695	2934	10.64	1.72
Mrk 110	1.0	10800	4	2.9	5.1	1775	1462	10.00	1.33
Mrk 198	2.0	7220	1	9.2	9.1	51	51	7.71	0.88
Mrk 231	1.0	12300	4	3.9	4.2	3459	3394	9.08	1.28
Mrk 266	2.0	8400	1	4.5	12.5	20	17	7.73	0.91
Mrk 268	2.0	12300	1	4.2	8.9	75	62	7.76	0.91
Mrk 273	2.0	11400	1	4.5	26.3	17	10	7.77	0.90
Mrk 290	1.0	9240	4	2.6	5.0	821	630	9.22	1.32
Mrk 291	1.0	10500	3	3.5	5.7	164	144	8.69	1.02
Mrk 315	1.5	11830	3	2.6	4.9	230	186	8.94	1.10
Mrk 335	1.0	7500	4	2.8	4.7	3457	3016	9.27	1.49
Mrk 372	1.5	9300	3	3.1	5.9	308	255	8.20	0.96
Mrk 382	1.0	10200	4	2.9	4.8	534	456	10.02	1.26
Mrk 423	1.9	9720	2	4.8	7.8	148	137	7.75	0.90
Mrk 474	1.0	12300	4	2.8	5.2	330	260	8.66	1.15
Mrk 477	2.0	11220	2	5.0	6.9	111	106	7.80	0.94
Mrk 486	1.0	11700	4	2.3	2.5	1905	1833	9.65	1.67
Mrk 493	1.0	9900	4	2.6	4.8	601	493	9.58	1.24
Mrk 506	1.5	12981	3	2.6	4.8	322	273	8.79	1.13
Mrk 509	1.0	10650	4	2.5	4.6	3446	2758	9.61	1.61
Mrk 516	1.8	8545	1	4.3	9.5	91	74	7.78	0.92
Mrk 530	1.0	8800	4	3.0	5.3	1188	963	7.88	1.16
Mrk 533	2.0	8620	3	3.3	5.9	274	241	7.54	0.95
Mrk 541	1.0	12300	1	5.3	7.7	72	68	8.40	0.90
Mrk 543	1.0	7800	4	2.9	5.4	400	322	9.84	1.10
Mrk 590	1.5	8100	4	2.7	4.9	708	614	8.06	1.07
Mrk 595	1.0	8400	4	2.7	4.9	860	746	8.24	1.13
Mrk 609	1.8	9600	2	3.6	6.7	265	223	8.54	0.92
Mrk 612	2.0	6066	1	7.4	10.1	54	52	7.16	0.89
Mrk 618	1.0	10200	4	2.6	4.9	1254	978	9.27	1.36
Mrk 622	2.0	6925	2	4.8	7.1	266	250	8.45	0.98
Mrk 699	1.0	10110	4	3.0	5.2	354	305	8.51	1.10
Mrk 704	1.0	8930	4	2.5	4.4	2033	1755	9.39	1.48
Mrk 766	1.0	3850	4	2.5	4.3	2558	2264	9.53	1.58
Mrk 817	1.0	9450	4	2.8	5.0	1590	1281	8.77	1.37
Mrk 841	1.2	10930	4	3.3	5.4	1222	1035	7.68	1.24
Mrk 871	1.0	9980	4	2.7	5.1	395	316	9.30	1.13
Mrk 1018	1.0	12810	4	3.2	5.2	544	493	8.31	1.14
Mrk 1040	1.5	4910	4	2.9	5.0	899	743	8.59	1.27
Mrk 1044	1.0	4920	4	3.1	4.9	1535	1381	7.93	1.28
Mrk 1048	1.5	12950	4	2.5	4.3	1849	1638	11.31	1.58
Mrk 1095	1.0	9900	4	2.9	5.2	3758	3023	8.61	1.31
Mrk 1146	1.0	11850	4	2.5	4.7	343	301	10.32	1.20
Mrk 1509	1.5	4990	4	2.9	4.9	2248	1852	9.26	1.37
Mrk 1514	1.0	5020	4	2.5	4.6	3662	2859	9.91	1.45
NGC 1019	1.0	7251	2	3.5	6.2	132	112	8.56	0.94
NGC 1358	2.0	4071	1	4.6	8.5	34	33	7.72	0.88
NGC 1409	2.0	7380	2	...	11.1	20	20	7.73	1.00
NGC 1667	2.0	4578	1	3.8	8.7	37	31	8.40	0.91
NGC 4074	2.0	6600	1	4.2	7.3	79	70	8.40	0.91

TABLE 2

B. NUCLEAR PROFILE PARAMETERS FOR MARKARIAN NON-SEYFERT GALAXIES

Name	cz km/s	*NPC*	*W*(2) pix	*W*(6) pix	*P*(2) DN	*P*(6) DN	*S*(2) (×100)	*S*(6)
(1)	(2)	(3)	(4)	(5)	(6)	(7)	(8)	(9)
Mrk 38	10823	1	8.7	9.8	22	22	8.38	0.94
Mrk 74	11536	1	5.9	11.1	11	10	7.18	0.91
Mrk 84	6300	3	3.0	5.7	164	133	8.13	0.99
Mrk 96	6600	2	2.8	17.6	14	6	7.95	0.93
Mrk 101	4837	2	3.1	6.2	46	36	8.60	0.90
Mrk 102	4296	3	2.6	5.6	155	110	7.76	0.99
Mrk 127	11100	1	4.6	8.5	59	54	7.78	0.90
Mrk 135	12900	2	4.7	7.9	56	51	8.39	0.93
Mrk 144	8269	1	7.6	14.1	9	7	7.76	0.89
Mrk 154	12900	1	7.8	9.2	14	13	7.19	0.88
Mrk 162	6300	0	3.5	9.1	18	13	7.29	0.90
Mrk 168	10200	0	5.9	10.7	7	6	8.76	0.93
Mrk 185	3000	1	23.1	14.9	14	13	7.72	0.92
Mrk 212	6900	1	5.3	8.3	122	113	8.39	0.91
Mrk 246	12300	0	4.8	12.2	8	6	7.32	0.90
Mrk 248	10800	...	...	...	...	...	...	...
Mrk 254	9000	1	5.4	22.5	11	7	7.75	0.89
Mrk 275	8100	1	3.2	9.2	15	10	9.20	0.90
Mrk 280	11200	...	...	...	...	...	...	...
Mrk 289	12000	0	...	12.9	20	19	7.73	0.88
Mrk 297	4800	1	3.9	7.7	11	9	7.28	0.91
Mrk 303	7500	1	4.8	9.2	21	18	8.37	0.92
Mrk 306	5700	0	8.4	16.2	4	4	8.70	0.96
Mrk 311	9300	1	5.5	9.6	44	39	7.78	0.89
Mrk 312	9900	1	5.2	9.1	16	15	7.78	0.91
Mrk 316	12300	3	2.7	4.8	181	159	10.03	1.16
Mrk 322	8100	2	5.5	8.1	75	70	8.36	0.91
Mrk 334	6900	4	3.0	5.6	645	529	8.93	1.11
Mrk 385	8100	2	3.9	8.0	57	44	8.49	0.93
Mrk 390	7200	1	4.5	8.0	40	35	7.75	0.89
Mrk 413	11537	3	3.5	6.0	104	88	7.97	0.97
Mrk 417	9721	2	2.7	8.0	80	43	8.72	0.90
Mrk 420	12858	2	4.9	7.5	53	48	7.75	0.89
Mrk 434	9840	1	9.3	10.3	29	26	7.71	0.88
Mrk 455	10238	3	3.0	5.3	47	39	7.78	1.04
Mrk 484	11700	0	...	9.2	6	8	7.26	0.92
Mrk 518	9750	2	3.5	6.6	75	68	8.50	0.92
Mrk 523	7950	1	5.9	8.5	77	74	7.18	0.88
Mrk 542	7500	1	4.7	15.3	25	18	8.38	0.89
Mrk 545	4804	2	5.0	8.9	113	102	7.17	0.91
Mrk 567	10050	3	2.9	5.8	164	142	7.59	0.92
Mrk 569	10050	1	3.8	6.4	35	32	7.26	0.89
Mrk 591	12450	1	4.8	7.8	73	66	7.77	0.91
Mrk 599	8878	0	4.6	...	6	4	8.49	0.91
Mrk 623	12562	0	6.6	9.2	71	65	8.47	0.95
Mrk 629	9601	3	3.4	7.0	37	30	7.82	0.89
Mrk 639	9960	1	...	27.9	2	3	8.04	0.91
Mrk 649	7053	2	7.6	9.2	265	258	7.71	0.92
Mrk 667	4950	1	10.4	9.9	16	16	8.36	0.92
Mrk 695	10590	1	3.7	7.9	40	33	7.88	0.93

1.0–1.5 galaxies (*upper histograms*) to have dominant point source nuclei (NPC = 4), while Seyfert 2 and non-Seyfert Markarian nuclei (*lower histograms*) tend to be weaker and resolved (NPC ~ 1). Using Student's *t*-test to compare the Seyfert 1 and 2 distributions (*top two panels*) we found a 5×10^{-11} probability that both have the same mean. By contrast, the Seyfert 1 and 1.5 distributions have the same mean at the 90% confidence level. The histograms of Seyfert 2 and non-Seyfert Markarian galaxies (*bottom two panels*) have a 25% chance of having the same mean.

3.2. *Quantitative Measures*

Admittedly, NPC is rather subjective, and a quantitative approach is desired to verify this striking distinction between Seyfert 1 and 2 nuclei. We have therefore made

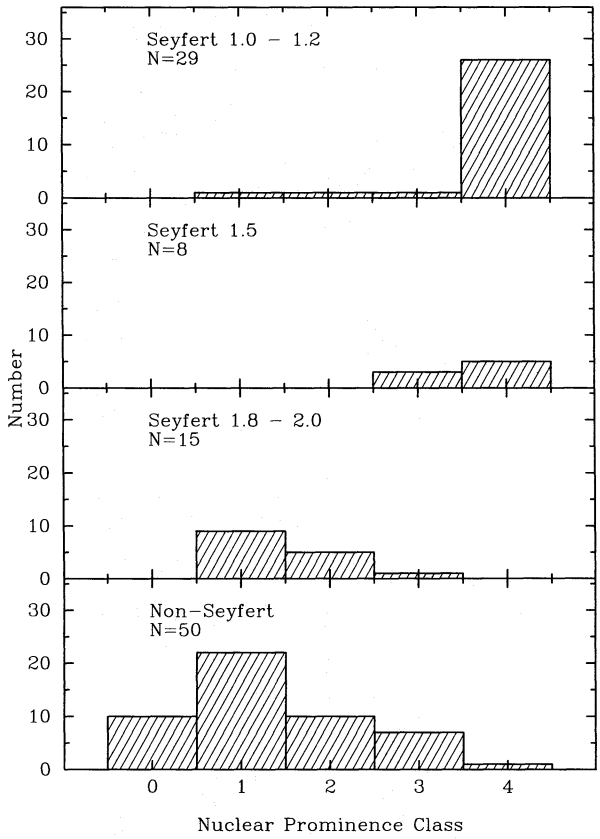

FIG. 2.—The distributions of the nuclear prominence class (NPC, defined in Table 1) are shown for different Seyfert types and for the non-Seyfert Markarian galaxies. Note the tendency for the type 1.0–1.5 Seyfert nuclei to be dominated by strong point sources (NPC = 4) while a large majority of the Seyfert 2 and non-Seyfert Markarian nuclei are weak and resolved (NPS = 1).

measurements of simple parameters characterizing the nuclear profiles. This provides a quantitative test of the morphological characterization in our NPC.

To provide a reference for our measurements we have constructed a model galaxy. The model uses a de Vaucouleurs $R^{1/4}$ law bulge with an $R_e = 2$ kpc, an exponential disk with a scale length $R_0 = 4$ kpc, and a bulge-to-total light ratio, $B/T = 0.3$. These parameters were chosen to be similar to those obtained from surface photometry of normal spirals (e.g., Kent 1985). Also, the disk scale lengths measured by MacKenty (1990) from ground-based images of the Seyfert sample are similar to the value in our model. The galaxy was taken to be face-on at a redshift of 9000 km s^{-1}, close to the mean of the Seyfert sample. A model PSF was constructed using the version 4.0 of the TinyTim package (Krist 1995) assuming a spacecraft rms motion or jitter of 15 mas.

3.2.1. *Gaussian Fits*

Gaussians were fitted to each undeconvolved nucleus, including points whose centers fell within circular apertures with radii of 2, 3, 4, 5, and 6 pixels. The correspondence between the fit and the profile was generally improved by subtracting a constant background level, determined as the median value in an annular region with inner and outer radii of 10 and 12 pixels (0.″43 and 0.″52). Ideally, the luminosity profile should be modeled using a careful separation of the bulge, disk, and nuclear components. Such an analysis will be presented in a forthcoming paper. At this stage, however, we prefer to keep the analysis simple. As we will show the results considered here are insensitive to the details of the fit.

For objects without strong point sources, the best Gaussian fits to the nuclear profiles were produced using the larger apertures and our background correction. However, the WF/PC-1 PSF has a bright ring that peaks between 3 and 4 pixels from the center (see Fig. 3). Thus, the best fits for objects with strong point sources were obtained using the smallest aperture, effectively excluding the light in the ring. In Tables 2A–2B we therefore present the FWHM measurements obtained in both the 2 and the 6 pixel radius apertures, $W(2)$ and $W(6)$, and the peak of the fit $P(2)$ and $P(6)$, using our simple corrections for the host galaxy background. Ellipses in the table columns indicate undetermined values.

In Figure 3, undeconvolved nuclear profiles are plotted for representative objects from each Seyfert class and the non-Seyfert Markarian galaxies. Each panel shows the Gaussian fit as a solid curve and the background level as a dashed line. For the strong point source objects, the fit using the 2 pixel radius aperture is shown since this gave a distinctly better match to the core of the profile than the larger apertures. For the other objects the 6 pixel radius fit is shown. The two horizontal bars at zero show the extent of circular aperture and the background annulus used for the fit. The interval selected for determining the background level is clearly arbitrary. The resulting FWHM and the sharpness parameter (see § 3.2.2.) in the 6 pixel radius aperture are given in the upper right.

We emphasize that these are typical profiles of our undeconvolved images and not extreme cases. The nuclei of Mrk 9, a Seyfert 1, and Mrk 1048, a Seyfert 1.5, are unresolved and show high peak counts relative to their underlying galaxies. The PSF ring peaking between 3 and 4 pixels in radius is clearly seen in these objects and in the model PSF. The nuclei of Mrk 477, a type 2 Seyfert, and Mrk 523, a non-Seyfert Markarian galaxy, are similar to the profiles of the model galaxy in being somewhat resolved and having significantly lower peak brightnesses Also, the PSF ring is not seen in these galaxies. We note that Mrk 9 and Mrk 477 have similar redshifts (12,040 km s^{-1} and 11,220 km s^{-1}, respectively) removing physical scale as an issue in this example diagram.

Because of the difficulty in fitting Gaussians to strong point sources using the larger apertures, we have compared the profile widths using just the 2 pixel aperture results, $W(2)$, just the 6 pixel aperture results, $W(6)$, and a mixture of the two which uses $W(2)$ for the unresolved nuclei and $W(6)$ for the rest of the sample. Figure 4 shows the distribution of widths using the mixed apertures. We prefer this method since it ensures that the profiles are faithfully represented by the fits and thus gives the best estimates of the size of the nucleus. We have also excluded eight non-Seyfert galaxies with peak heights less than 10 DN over the background for which the Gaussian fits are not reliable.

Figure 4 shows that the nuclei of the types 1–1.5 Seyfert galaxies in the sample are predominantly unresolved point sources. The Seyfert 1 distribution has a median FWHM of 2.8 pixels, comparable to that for the WF/PC-1 point spread function and for stars seen in our snapshot images. An arrow indicates the width measured from a Gaussian fit

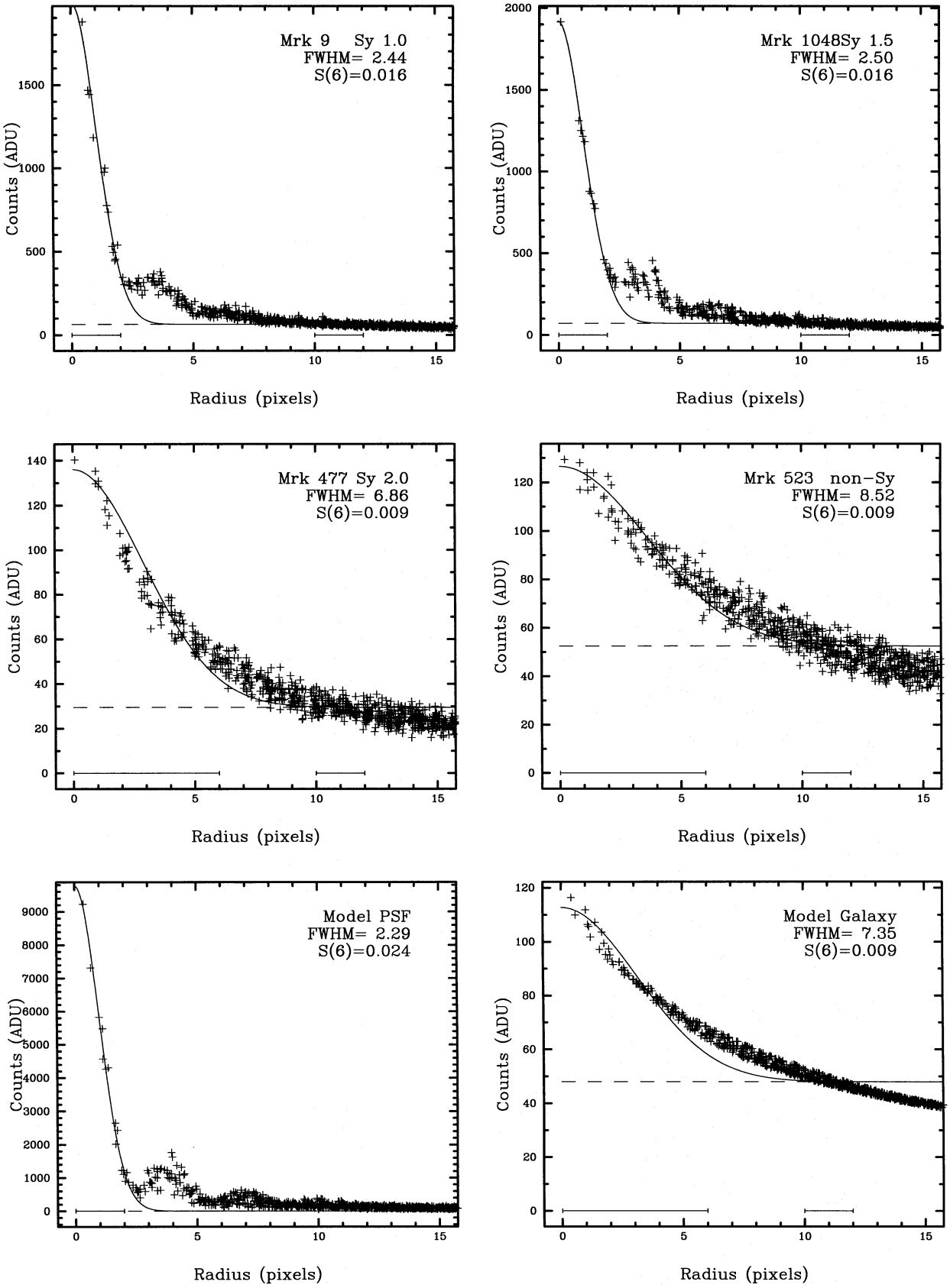

FIG. 3.—Radial profiles are shown for representative objects from each class. The solid curve shows a Gaussian fit and the dashed line shows the level of a constant background subtracted before the fit. The horizontal bars at 0 counts indicate the range of points used in the fit and the determination of the background level. Note the appearance of the PSF ring peaking between 3 and 4 pixels radius in the unresolved Seyfert nuclei and the model PSF. A smaller aperture fit produced better results in the objects displaying this feature.

to the model PSF. Only one Seyfert 1, Mrk 541, shows a resolved nuclear source. The Seyfert 1.5 nuclei have a similar distribution with a mean FWHM of 2.7 pixels. Student's t-test gives a 10% probability of having the same mean as the type 1 Seyfert galaxies.

The Seyfert 2 nuclei in Figure 4 are found to be generally broader, with a mean FWHM of 9.1 pixels, and have a much larger range of values. There is only a 0.08% probability of the same mean as the type 1 Seyfert galaxies. The non-Seyfert Markarian galaxies also have a broad distribution of profile widths with a mean FWHM of 6.8 pixels and 16% probability of the same mean as the type 2 Seyferts. Thus, using a quantitative measure of the shape of the nuclear profiles we find a distinct difference between the types 1 and 2 Seyferts. We have also marked the position of our model galaxy on the diagram. Interestingly, it is similar to the typical widths for both the type 2 Seyferts and the non-Seyfert Markarian galaxies. The results obtained by comparing the distributions without subtracting a background level, using just $W(2)$, or using just $W(6)$ are the same (see Table 3). The individual values change with the fit parameters but the separation between Seyfert 1 and 2 galaxies remains.

Figure 5 shows the widths of the profiles as a function of redshift for the Seyfert 1.0–1.5 galaxies in the upper panel and the Seyfert 1.8–2.0 galaxies in the lower panel. Although the Seyfert 1 galaxies tend to be found at a higher redshift than the Seyfert 2 galaxies, one can see that the redshift distributions overlap considerably. Evidently the difference in the profile widths between Seyfert 1 and 2 galaxies cannot be attributed to differences in their redshift distributions. In both panels the lower dashed line represents an unresolved point source. The other dashed lines show the expected profile widths for a Gaussian shaped nucleus of 100 and 200 pc FWHM convolved with the WF/PC-1 PSF as a function of redshift. The plus sign at $cz = 9000$ km s^{-1} shows the expected width of our model galaxy.

We note that although spacecraft jitter may occasionally produce significant broadening of the observed PSF, it would be quite a coincidence for the jitter to be large when observing type 2 Seyferts and always low for type 1 Seyferts. We have checked against this possibility by measuring the widths of stars in both the images of Seyfert 1 and 2 galaxies and found them both to be quite comparable to the widths measured for Seyfert 1 nuclei. From these measurements it is apparent that jitter is always less than 50 mas and usually less than 30 mas, ruling out jitter as a significant influence on the nuclear profiles. Furthermore, we have verified that the ordering of the observations was well mixed with regards to Seyfert type so that systematic changes in the telescope over time have not affected our results.

3.2.2. *Sharpness Measurements*

The nuclear sharpness, S, another parameter characterizing the profile shape, is sensitive to the contrast in the pixel values within a given aperture. The sharpness is defined within a circular aperture of a given radius as

$$S = \frac{\sum_i c_i^2}{(\sum_i c_i)^2}, \quad (1)$$

where c_i is the counts in analog-to-digital converter units in each pixel (Hasan 1994). The parameter ranges from $S = 1.0$ for a δ-function to $1/N$, for a flat, constant, surface, where N is the number of pixels used in the calculation. We have measured the sharpness parameter using apertures of radii of 2, 3, 4, 5, and 6 pixels on undeconvolved images that have been cleaned of cosmic rays. The sharpness parameter is more robust than the FWHM of a Gaussian fit since it makes no assumptions about the shape of the profile or the light from the underlying galaxy. In Tables 2A–2B we present the sharpness values for the 2 and 6 pixel apertures, $S(2)$ and $S(6)$.

The distributions of $S(2)$, nuclear sharpness in the 2 pixel radius aperture, are shown in Figure 6, again separating by Seyfert class. The generally low sharpness values for all classes reflect the aberrated nature of the *HST* WF/PC-1

TABLE 3

NUCLEAR PROFILE PARAMETERS FOR TYPES 1 AND 2 SEYFERT GALAXIES

	SEYFERT 1		SEYFERT 2		
PARAMETER (1)	Mean (2)	Standard Deviation (3)	Mean (4)	Standard Deviation (5)	STUDENT'S t-TEST P (null) (6)
NPC	3.66	0.97	1.47	0.64	$<10^{-7}$
Profile Widths					
$W(2)$, background subtracted	3.00 pixels	0.60 pixels	4.87 pixels	1.58 pixels	6.6×10^{-4}
$W(6)$, background subtracted	5.08	0.68	9.77	4.90	2.4×10^{-3}
W mixed, background subtracted	3.08	0.98	9.06	5.42	8.4×10^{-4}
$W(2)$	3.23	0.87	6.86	2.67	1.9×10^{-4}
$W(6)$	5.92	1.31	15.45	9.39	1.5×10^{-3}
W mixed	3.54	1.88	15.19	9.66	3.6×10^{-3}
Sharpness					
$S(2)$	0.090	0.007	0.079	0.004	$<10^{-7}$
$S(6)$	0.013	0.002	0.009	0.001	$<10^{-7}$
$S(2)$, background subtracted	0.093	0.008	0.081	0.004	1.3×10^{-7}
$S(6)$, background subtracted	0.016	0.002	0.011	0.001	$<10^{-7}$

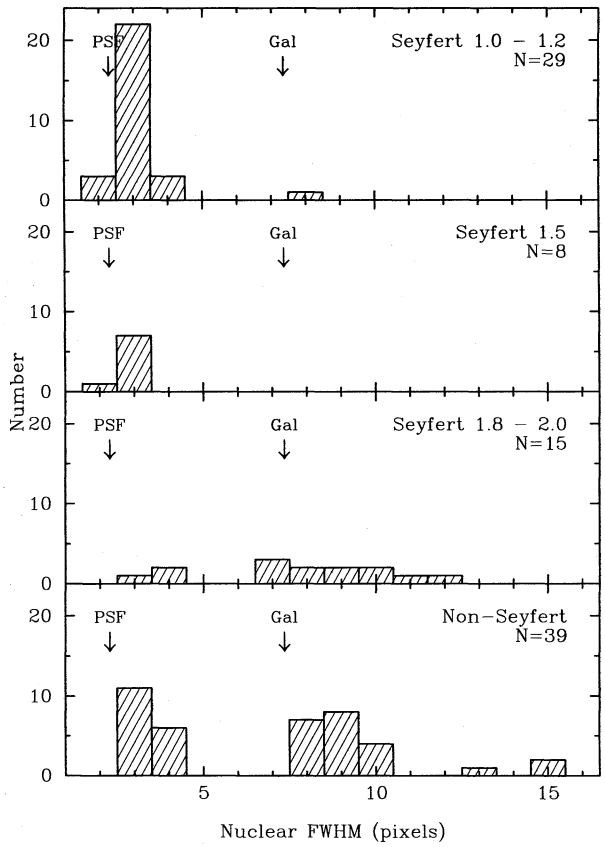

FIG. 4.—Distributions of the nuclear FWHM for the different Seyfert types and the non-Seyfert Markarian galaxies. The widths of a model PSF produced by TinyTim and a model galaxy (see text) are indicated with arrows. Note the narrow unresolved widths of the types 1.0–1.5 Seyferts in contrast to the extended profiles of the Seyfert 2 and non-Seyfert Markarian Galaxies. Gaussian fits were made to points within 2 pixels of the center for the point source nuclei and within 6 pixels for the resolved objects. A constant background level determined as the mean of the points in an annulus with inner and outer radii of 10 and 12 pixels was subtracted before fitting.

point-spread function. Clearly, the type 1 Seyfert galaxies tend to have "sharper" nuclei than the Seyfert 2 galaxies. Student's t-test gives the probability of both distributions having the same mean as less than 10^{-7}. The sharpness distribution for the type 1.5 Seyferts is similar to that for the type 1 Seyferts with a 60% probability of the same mean. The fact that the types 1.0–1.5 Seyferts are not as sharp as the model PSF can be attributed to the lack of underlying galaxy in the latter or a slightly higher degree of spacecraft jitter. Tests show that by adding a constant background or by increasing the amount of jitter from 15 to 30 mas the sharpness of the model PSF can be reduced to values typical of the type 1 Seyferts. The distributions for the Seyfert 2 and non-Seyfert Markarian galaxies have mean values that are not very different from that of our model galaxy and have a 36% likelihood of having the same mean. We have performed the same analysis including a background correction and using different apertures sizes (see Table 3). The basic trends are again the same; nuclei of types 1.0–1.5 Seyferts are distinctly sharper than those of type 2 Seyferts and the non-Seyfert Markarian galaxies.

4. DISCUSSION

There is a clear distinction between the types 1 and 2 Seyferts using any of several different schemes to classify or quantify the nuclear profile shapes. As was mentioned in the previous section, while a careful decomposition of the luminosity profile into bulge, disk, and nuclear components is required to obtain accurate nuclear magnitudes and sizes, such an approach is unnecessary to distinguish between point sources and resolved nuclei. A summary of the results of the different parameters used in this paper is given in Table 3. For each parameter, the mean and standard deviation for types 1.0–1.5 Seyferts and for the types 1.8–2.0 Seyferts is given and the probability of the same mean from Student's t-test. Although the values obtained for the profile widths and sharpnesses change with the aperture used to estimate them, the difference between the Seyfert 1 and 2 galaxies as distinct groups persists. The same is true for the results whether or not a background level is subtracted.

Thus, the results presented in § 3 suggest a significant difference in the nature of the nuclei observed in types 1 and 2 Seyferts. Seyfert 1 nuclei are bright and essentially unresolved, not only at the resolution of ground-based studies, but also with the 5–10 times higher resolution of the *HST*. This is consistent with these being the directly observed ionizing continuum source. Seyfert 2 nuclei are less distinct and are similar in shape to the central regions of normal galaxies.

In unified models of AGNs the nuclear continuum in type 2 Seyfert galaxies is blocked by a dense torus of molecular gas. It can be seen only as light scattered into our line of sight by material that has a direct view of the nucleus, lying in a region above the opening of the torus. Our results are consistent with this prediction in that any nuclear *point source* is either extremely weak or absent in our observations of type 2 Seyferts. However, observations have suggested that the scattering regions and therefore the observed continua of type 2 Seyferts are extended (e.g., NGC 1068; Antonucci, Hurt, & Miller 1994). To address this issue we must first consider whether any of the scattered continuum is detected in our images. It may be that the nuclear continua, which are strong in the ultraviolet, are simply too weak to be detected in our bandpass in the near-infrared where the relative contribution from the underlying galaxy is increasing.

Estimates of f_c, the fraction of the total light within some aperture emitted as featureless continuum, have previously been obtained using several different techniques. These include extrapolation of UV spectra to optical wavelengths (Kinney et al. 1991), scaling of template elliptical galaxy spectra to match the strength of observed stellar absorption features (e.g., Koski 1978; Miller & Goodrich 1990; Tran 1995a), and measurement of the dilution of optical and infrared stellar absorption lines (Terlevich, Diaz, & Terlevich 1990; Nelson & Whittle 1996). These spectroscopic studies find somewhat different results for individual objects, largely reflecting the uncertainties of each technique. Also, the analysis is clearly aperture dependent since the host galaxy light is extended and Seyfert 2 nuclei are unresolved from the ground. Thus, for any given object, increasing the aperture size will decrease the value of f_c. Also, for more distant objects, a larger portion of the host galaxy will fall within a fixed aperture. Nevertheless, these studies all find a similar but broad range of values, with $f_c \sim 30\%$ at 5000 Å.

Since the flux per unit wavelength from an old stellar population is essentially flat between 5000 and 10,000 Å ($f_\lambda \simeq$ const.; see, e.g., Bica & Alloin 1987), the relative con-

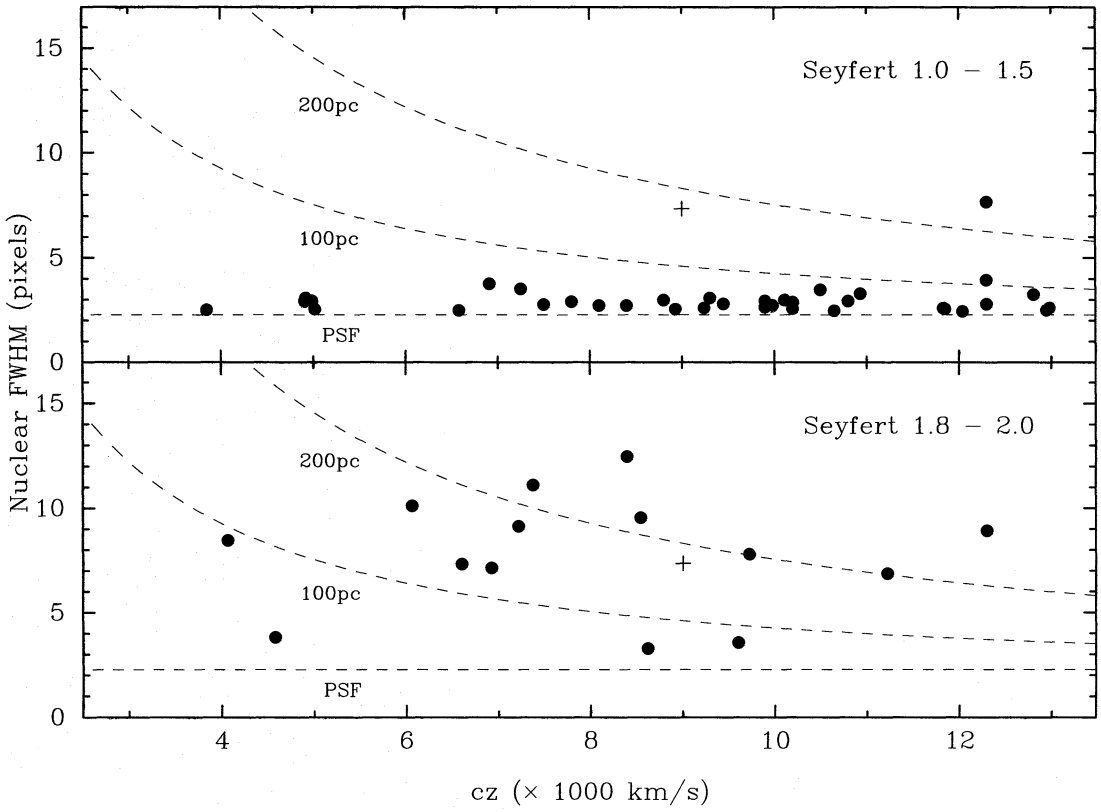

FIG. 5.—Nuclear FWHM from Gaussian fits shown in Fig. 4 is plotted as a function of redshift for type 1.0–1.5 Seyferts in the upper panel and for the type 2 Seyferts in the lower panel. The differences between the two types are not due to differences in redshift distribution. The dashed lines indicate the widths expected for fits to Gaussian profiles with FWHM of 100 and 200 pc convolved with the PSF and are provided for scale reference.

tribution from a power-law continuum, $f_\lambda \propto \lambda^{-\gamma}$, should also be proportional to $\lambda^{-\gamma}$. Taking $\gamma = 0.5$ (corresponding to $f_\nu \propto \nu^{-1.5}$) to be a typical value for Seyfert galaxies (e.g., Kinney et al. 1991), we expect f_c to decrease by only roughly 25% from the visual to our bandpass. Thus, we still expect a sizable contribution to the nuclear flux from the featureless continuum in our images.

Using our model galaxy we can simulate the effect of the featureless continuum source on our analysis by adding nuclear components of varying relative strengths and sizes. In Figure 7*a* the change in the FWHM in the 6 pixel radius aperture is shown as a function of f_c for a point source nuclear component and an extended nuclear source that consists of a 50 pc FWHM Gaussian ($cz = 9000$ km s^{-1} for the model) convolved with the WF/PC-1 PSF. The value of f_c has been evaluated in a 0.″5 radius, actually somewhat smaller than the apertures used in the ground-based spectroscopic studies discussed above. For values of $f_c > 0.1$, the addition of the point source component has caused the profile width to drop well below the mean value for the Seyfert 2 galaxies in Figure 4 and rapidly approaches that of the Seyfert 1 galaxies. The width of the extended source also decreases with increasing f_c, but never diminishes to the widths observed for the type 1 Seyferts since they are truly unresolved. Figure 7*b* shows the expected change in the sharpness in a 2 pixel radius aperture as a function of f_c. A similar effect is seen; the sharpness increases with f_c much more quickly for the unresolved nuclear component than for the extended source.

We notice that the width of the extended source is also significantly below the mean width for the type 2 Seyferts, suggesting that the continuum sources in these objects may often be quite large. This is supported by recent observations and modeling of the nearby Seyfert 2 galaxy NGC 1068, where the scattering "mirror" may be extended over as much as 1″ (Miller, Goodrich, & Mathews 1991; Caganoff et al. 1991; Antonucci, Hurt, & Miller 1994). Recent imaging polarimetry of NGC 1068 by Capetti et al. (1995) has found evidence for scattered nuclear continuum emission as far as 9″ from the center of the galaxy. Other evidence of extended scattering mirrors in Seyfert 2 galaxies has been found in off-nuclear spectroscopy of NGC 4388 by Shields & Filippenko (1988). They detected broad Hα emission as much as 4″ away from the apparent nucleus. Using *HST* images of the Seyfert 2 galaxy Mrk 463E, Uomoto et al. (1993) have detected an optical "jet" 0.″84 long, which may be largely scattered nuclear continuum emission. Tran (1995b) has also detected off-nuclear polarization mirrors in Mrk 463E ~ 2″ from the center, much like those seen in NGC 1068. This detection has now been confirmed with better resolution polarimetric imaging data from the Keck telescope (H. D. Tran, private communication).

Also diffuse near-UV continuum emission has recently been detected from the ground in the centers of two Seyfert 2 galaxies by Pogge & De Robertis (1993).

The simulations and the results of the previous section

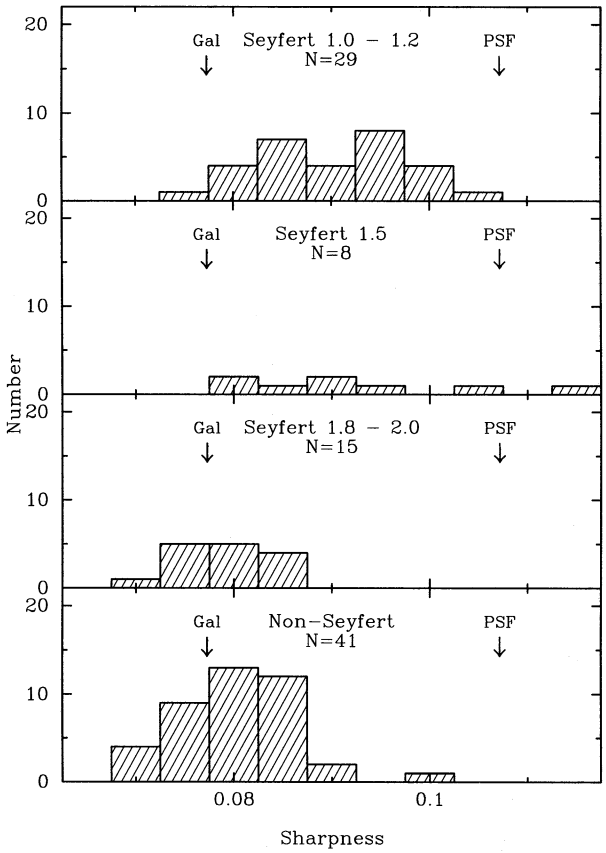

FIG. 6.—The sharpness in a 2 pixel radius aperture for the different classes of objects is plotted as a histogram. Arrows indicate the sharpnesses of a model galaxy and a TinyTim point spread function. The Seyfert 1.0–1.5 nuclei show a much larger range and a higher mean value than the type 2 and non-Seyfert Markarian galaxies.

suggest two possibilities for the type 2 Seyfert galaxies in our sample. Either their nuclear continua are considerably weaker than expected from previous spectroscopic studies that separated nonthermal and stellar components or they tend to be extended sources that blend in with the luminosity profile of the host galaxy. We consider the first possibility unlikely since our simulations have used a conservative aperture of radius 0".5 and the spectroscopic work has reached the same conclusions by rather independent techniques. Thus, we are driven to conclude that the featureless nuclear continuum in Seyfert 2 galaxies must be extended in accord with the predictions of AGN unification models.

A puzzling case is the Seyfert 2 galaxy Mrk 477. Kinney et al. (1991) reported it to have a variable continuum, suggesting a compact electron scattering region (<1 pc; Antonucci 1992). In contrast, Tran (1992b) and Veilleux (1988) have found no evidence for variability in Fe emission lines. Our observations show that this object has a reasonably soft, slightly resolved nucleus indicating an extended continuum source. Either the continuum source is not variable or our snapshot image was taken while it was weak and any contribution from an unresolved component was small.

Interestingly, the results from § 3 show that the nuclear profiles of the type 1.5 Seyferts are indistinguishable from the Seyfert 1 nuclei. This suggests that the nuclear continuum emission in these objects, although partially obscured, is still dominated by a directly viewed unresolved nuclear component. The three objects of types 1.8 and 1.9 in our sample follow the distributions of the Seyfert 2 galaxies, which suggests that although some of the BLR is visible directly, it is the scattered continuum source that is much stronger.

Recent work by Tran (1995c) has suggested that the continua in Seyfert 2 galaxies may also contain a substantial contribution from an unpolarized and hence directly viewed component, F_{c2}, comprising $\sim$60%–90% of the total featureless nuclear continuum. The origin of this emission is still in question, and possible explanations include optically thin thermal radiation from the scattering medium and a circumnuclear starburst. In either of these scenarios, the F_{c2} emission would be spatially extended. Heckman et al. (1995) have reexamined the ultraviolet continua of Seyfert 2 galaxies by forming a template spectrum composed of 20 of the brightest Seyfert 2 galaxies. They conclude that a large fraction of the energetics of these objects is due to nuclear starburst activity. The similarity in the profiles of the Seyfert 2 and non-Seyfert Markarian galaxies suggests that the observed nuclei of Seyfert 2 galaxies may contain a significant contribution from a circumnuclear starburst. A starburst component may also be present in the Seyfert 1 galaxies in our sample but would be masked by the strong point source.

5. CONCLUSIONS

We have examined the nuclei of Seyfert and non-Seyfert Markarian galaxies from our *HST* snapshot survey. We find that the nuclei of type 1 Seyfert galaxies are generally dominated by a strong point source while those of type 2 Seyfert galaxies are often resolved by *HST*, are considerably weaker, and have profile shapes similar to the bulges of normal galaxies. We also find that the nuclear profiles of the Seyfert 1.5 galaxies are indistinguishable from the type 1 Seyferts. The nuclei of the non-Seyfert Markarian galaxies often resemble those of type 2 Seyferts. These observations are consistent with the expectations from unified models for AGNs, in which the ionizing continuum source is viewed directly in the nuclei of type 1 Seyferts and is seen only as an extended source of scattered light in the type 2 Seyferts. It is also possible that the nuclear regions of Seyfert 2 galaxies are similar to those of non-Seyfert Markarian galaxies, where a starburst is likely the main contributor to the observed nuclear emission.

Support for this work was provided by NASA through grants GO05-70600 and GO05-97900 from the Space Telescope Science Institute, which is operated by the Association of Universities for Research in Astronomy, Inc., under NASA contract NAS 5-26555. It is a pleasure to thank Gina Jones for her help with the data reduction and analysis. We would also like to thank Bob Goodrich, Anne Kinney, Alessandro Capetti, and Chris Simpson for helpful discussions and the referee, Hien Tran, for his useful comments.

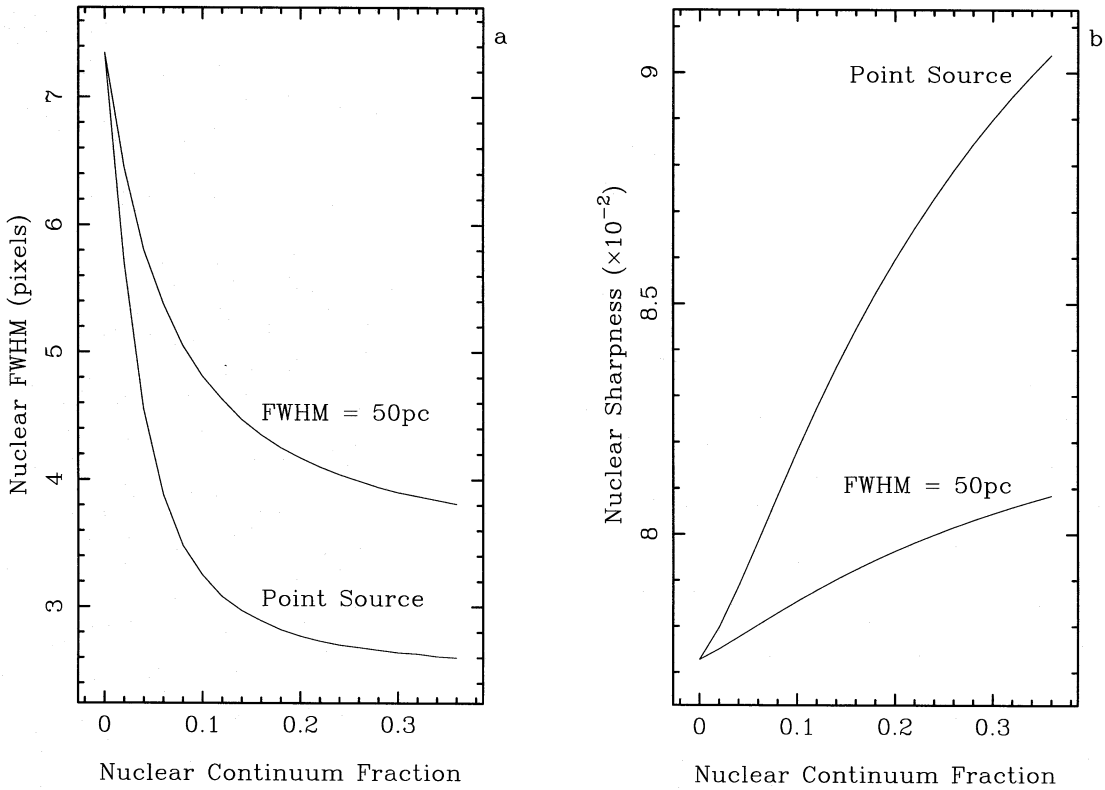

FIG. 7.—Simulated nuclear profiles were constructed using a model galaxy and two different nuclear components: one unresolved and the other an extended Gaussian. The effects on the profile widths (*a*) and sharpness parameters (*b*) produced by increasing the fraction of light in the nuclear component are shown. The nuclear continuum fraction, f_c is taken as the ratio of the light due to the nuclear component to the total light in a 1″ diameter aperture. In the point source case, the nuclear component clearly dominates the profile shape for values of $f_c > 0.1$, while the extended source has a significantly smaller impact.

REFERENCES

Antonucci, R. 1993, ARA&A, 473, 31
Antonucci, R., Hurt, T., & Miller, J. 1994, ApJ, 430, 210
Antonucci, R. R. J. 1992, in AIP Conf. Proc., No. 254, Testing the AGN Paradigm, ed. S. S. Holt, S. G. Neff, & C. M. Urry (New York: AIP), 486
Antonucci, R. R. J., & Miller, J. S. 1985, ApJ, 297, 621
Bica, E., & Alloin, D. M. 1987, A&A, 186, 49
Caganoff, S., et al. 1991, ApJ, 377, L9
Capetti, A., Macchetto, F., Axon, D. J., Sparks, W. B., & Boksenberg, A. 1995, ApJ, 448, 600
Hasan, H. 1994, Instrument Science Rep., No. OTA 16, April 19
Heckman, T., et al. 1995 ApJ, 448, 98
Kent, S. M. 1985, ApJS, 59, 115
Kinney, A. L., Antonucci, R. R. J., Ward, M. J., Wilson, A. S., & Whittle, M. 1991, ApJ, 377, 100
Koski, A. T. 1978, AJ, 223, 56
Krist J. E. 1995, in ASP Conf. Ser., Vol. 77, Astronomical Data Analysis Software and Systems IV, ed. R. A. Shaw, H. E. Payne, & J. J. E. Hayes (San Francisco: ASP), 349
Lauer, T. R. 1989, PASP, 101, 445
Lucy, L. B. 1974, AJ, 79, 745
MacKenty, J. W. 1989, ApJ, 343, 125 (Paper II)
———. 1990, ApJS, 72, 231 (Paper I)
MacKenty, J. W., et al. 1992, *Hubble Space Telescope* Wide Field/Planetary Camera Instrument Handbook (Baltimore: Space Science Telescope Inst.)
MacKenty, J. W., Nelson, C. H., Simkin, S. M., & Griffiths, R. E. 1996, in preparation (Paper III)
Miller, J. S., & Goodrich, R. W. 1990, ApJ, 355, 456
Miller, J., Goodrich, R. W., & Mathews, W. G. 1991, ApJ378, 47
Nelson, C. H., & Whittle, M. 1996, in preparation
Peterson, B. M. 1993, PASP, 105, 247
Pogge, R. W., & De Robertis, M. M. 1993, ApJ, 404, 563
Richardson, W. H. 1972, J. Opt. Soc. Am., 62, 55
Shields, J. C., & Filippenko, A. V. 1988, ApJ, 332, L55
Terlevich, E., Diaz, A. I., & Terlevich, R. 1990, MNRAS, 242, 271
Tran, H. D. 1995a, ApJ, 440, 565
———. 1995b, ApJ, 440, 578
———. 1995c, ApJ, 440, 597
Uomoto, A., Caganoff, S., Ford, H. C., Rosenblatt, E. I., Antonucci, R. R. J., Evans, I. N., & Cohen, R. D. 1993, AJ, 105, 1308
Veilleux, S. 1988, AJ, 95, 1695
Westphal, J. A., et al. 1982, The Space Telescope Observatory, ed. D. N. B. Hall, NASA: CP-2244, 28
Wilson, A. S. 1995, in Oxford Astronomy Workshop, Evidence for the Torus, ed. M. J. Ward (Oxford), 55